Evaluation of the nonlinear optical properties for an expanded porphyrin Hückel-Möbius aromaticity switch

Miquel Torrent-Sucarrat, Josep M. Anglada, and Josep M. Luis

Citation: J. Chem. Phys. **137**, 184306 (2012); doi: 10.1063/1.4765667
View online: http://dx.doi.org/10.1063/1.4765667
View Table of Contents: http://jcp.aip.org/resource/1/JCPSA6/v137/i18
Published by the American Institute of Physics.

Evaluation of the nonlinear optical properties for an expanded porphyrin Hückel-Möbius aromaticity switch

Miquel Torrent-Sucarrat,[1,a)] Josep M. Anglada,[1] and Josep M. Luis[2,b)]
[1]*Departament de Química Biològica i Modelització Molecular, Institut de Química Avançada de Catalunya (IQAC-CSIC), c/ Jordi Girona 18, E-08034 Barcelona, Spain*
[2]*Institut de Química Computacional and Departament de Química, Universitat de Girona, E-17071 Girona, Catalonia, Spain*

(Received 28 July 2012; accepted 19 October 2012; published online 9 November 2012)

The conformational flexibility of the expanded porphyrins allows them to achieve different topologies with distinct aromaticities and nonlinear optical properties (NLOP). For instance, it is possible to switch between Möbius and Hückel topologies applying only small changes in the external conditions or in the structure of the ring. In this work, we evaluate the electronic and vibrational contributions to static and dynamic NLOP of the Hückel and Möbius conformers of A,D-di-p-benzi[28]hexaphyrin(1.1.1.1.1.1) synthesized by Latos-Grażyński and co-workers [Angew. Chem., Int. Ed. **46**, 7869 (2007)]. Calculations are performed at the HF, M052X, and CAM-B3LYP levels using the 6-31G, 6-311G(d), and 6-31+G(d) basis sets. Our results conclude that M052X/6-31G and CAM-B3LYP/6-31G methods provide a correct qualitative description of the electronic and vibrational contributions for the NLOP of expanded porphyrins. The studied systems show high NLOP with large differences between the Möbius and Hückel conformations (around 1×10^6 a.u. for $\bar{\gamma}$). The obtained results indicate that the expanded porphyrins are promising systems to manufacture Hückel-to-Möbius topological switches. © *2012 American Institute of Physics*. [http://dx.doi.org/10.1063/1.4765667]

I. INTRODUCTION

Möbius aromaticity[1,2] has revolutionized the chemistry of expanded porphyrins. Sessler and Seidel[3] defined expanded porphyrins as "synthetic analogues of the porphyrins, and differ from these and other naturally occurring tetrapyrrolic macrocycles by containing a larger central core with a minimum of 17 atoms, while retaining the extended conjugation features that are a hallmark of these quintessential biological pigments." The conformational flexibility, the number and the nature of substituents on the pyrrolic and meso positions, and the metallation of the porphyrins allow them to achieve different topologies with distinct aromaticities, magnetic, and electric properties.[4] In the last five years several Hückel and Möbius topological systems have been prepared through replacement of the solvent and protonation,[5–7] temperature control,[8,9] metal coordination,[10] and functional group modifications.[11] As one can see, the synthesis of aromatic systems with Möbius topology has just started and there are still a lot of aspects and applications to be analyzed.

One of the most appealing applications is the possibility of designing new topologically switchable porphyrins with high nonlinear optical properties (NLOP).[12] The expanded porphyrins can exchange between the Hückel and Möbius topologies applying small changes in the external conditions (temperature, solvent, redox potential) or in the structure of the ring. The key factors, which will determine their potential use as optical switches are the high values of the NLOP and the large differences between the NLOP of the Möbius and Hückel conformations.

In the literature, there exist only a few works about the evaluation of the NLOP with Hückel and Möbius tolopologies. Xu *et al.*[13] studied the electronic dipole moment and first hyperpolarizability of aza-[7]cyclacenes with/without a knot and four knots isomers of strip aza-[15]cyclacenes. In addition, Wang *et al.*[14] reported the electronic first hyperpolarizability of a Möbius basket molecule based on six fused five-membered pyrrole rings. Wang *et al.*[15] described the lithium-effect on the NLOP in the short zigzag-edged monolithiated aza-Möbius grapheme ribbon [2,7] isomers. Finally, the present authors[16] studied the electronic and vibrational contributions to static and dynamic NLOP of the C_S Hückel and C_2 Möbius conformers of the bianthraquinodimethane modified [16] annulene synthesized by Herges and coworkers.[2] Calculations were performed at the HF, B3LYP, BHandHLYP, BMK, M052X, CAM-B3LYP, and MP2 levels with the 6-31+G(d) basis set. Our results concluded that BHandHLYP, M052X, and CAM-B3LYP methods correctly reproduce the x-ray crystal structure and provide similar nonlinear optical properties, which can be considered of a semiquantitative quality. Moreover, we found that the NLOP values for Hückel and Möbius conformations of the bianthraquinodimethane modified [16] annulene are very similar.

As far as we know, no analogous of NLOP calculations have been carried out for expanded porphyrins. This work is the first attempt to determine their potential as optical switches. We have carried out a complete evaluation of their electronic and vibrational contributions to static and

a)E-mail: miqueltorrentsucarrat@gmail.com. Telephone: +34 934006111. Fax: +34 932045903.
b)Telephone: +34 972418272. Fax: +34 972418356.

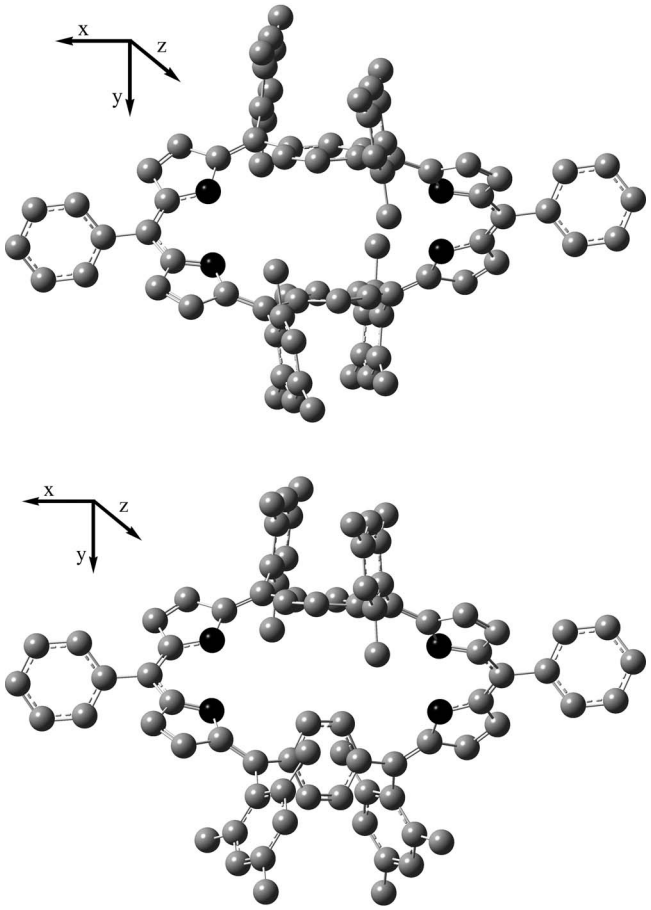

FIG. 1. CAM-B3LYP/6-311G(d) optimized geometries of Hückel (top, **1-H**) and Möbius (bottom, **1-M**) topologies of A,D-di-p-benzi[28]hexaphyrin(1.1.1.1.1.1). The hydrogen atoms have been omitted for clarity.

dynamic NLOP of both Hückel and Möbius conformers. The selected system is the first reported dynamic switch between Hückel and Möbius in a expanded porphyrin analogue containing para-phenylene rings, the A,D-di-p-benzi[28]hexaphyrin(1.1.1.1.1.1) (**1**; A and D denote the positions of the phenylenes rings in the macrocyclic structure) synthesized by Stepień *et al.* (see Figure 1).[5] This system shows solvent-dependent equilibrium between the Hückel, **1-H**, and Möbius, **1-M**, conformations. In some solvents, such as aliphatic hydrocarbons and alcohols, only **1-H** is observed. On the other hand, in solvents such as benzene or dichloromethane, a certain amount of **1-M** is also present. And finally, **1-M** becomes the dominant conformer in chloroform and *N,N*-dimethylformamide. In a more recent work, Stepień *et al.*[7] also found that this system is sufficiently flexible to switch between three distinct π-conjugation topologies planar Hückel (antiaromatic, **1-H**), singly twisted Möbius (aromatic, **1-M**), and double twisted Hückel (antiaromatic), without changing its oxidation level. This process is under both thermodynamic and kinetic reaction control and can be realized in three- or four-step cycle, which supports the potential practical value of these topological switches.

This article is organized as follows. Section II summarizes the methodological and computational considerations. It is followed in Sec. III by a discussion of the results obtained for the electronic and vibrational contributions to static and dynamic NLOP of **1-H** and **1-M** in gas phase and in solvent. Finally, our conclusions are given in Sec. IV.

II. COMPUTATIONAL METHODS

The evaluation of the static electronic contribution to dipole moment, μ^e, linear polarizability, α^e, first hyperpolarizability, β^e, and second hyperpolarizability, γ^e, were performed at the HF, M052X,[17] and CAM-B3LYP[18] levels with the 6-31G, 6-311G(d), and 6-31+G(d) basis sets[19] using the GAUSSIAN 09 program package.[20] μ^e, α^e, and β^e were analytically evaluated for all the methodologies. In contrast, γ^e was obtained by finite field differentiation of β^e. The numerical differentiation was carried out for field strengths of ± 0.0002, ± 0.0004, ± 0.0008, and ± 0.0016 a.u. The smallest field magnitude that produced a stable derivative was selected using a Romberg method triangle.[21] The symmetry restrictions have not been considered in the optimization process and the structures of **1-H** and **1-M** at B3LYP/6-31G(d,p) obtained by Stepień *et al.*[5] have been used as the initial geometry of the optimization process. The geometry optimizations in gas phase have been done at HF, M052X, and CAM-B3LYP levels with the 6-31G and 6-311G(d) basis sets. The average (hyper)polarizabilities are defined by following equations:[22]

$$\bar{\alpha} = \frac{1}{3} \sum_{i=x,y,z} \alpha_{ii}, \tag{1}$$

$$\bar{\beta} = \frac{1}{5|\bar{\mu}|} \sum_{i,j=x,y,z} \mu_i(\beta_{ijj} + \beta_{jij} + \beta_{jji}), \tag{2}$$

and

$$\bar{\gamma} = \frac{1}{15} \sum_{i,j=x,y,z} \gamma_{iijj} + \gamma_{ijij} + \gamma_{ijji}. \tag{3}$$

We have considered the solvation effect in the static electronic contribution to NLOP using the self-consistent reaction field (SCRF) approach[23] with a dielectric constant of benzene ($\varepsilon = 2.271$), chloroform ($\varepsilon = 4.711$), and ethanol ($\varepsilon = 24.852$). The polarizable continuum model using the integral equation formalism variant has been calculated using the radii and non-electrostatic terms of Truhlar and co-workers' SMD solvation model.[24] The geometry optimizations in solution have been done using the CAM-B3LYP approach with the 6-31G basis set.

The vibrational (hyper)polarizabilities can be computed using the pioneer perturbation treatment of Bishop and Kirtman (BK) (Refs. 25 and 26) or the variational approach based on analytical response theory proposed by Christiansen *et al.*[27] One approach intertwined to BK method is the nuclear relaxation approach, whose derivation of vibrational NLOP formulas is based on determining the change in the equilibrium geometry induced by a static external field.[28–30] Even though there is an exact correspondence between static and infinite optical frequency approximation vibrational hyperpolarizabilities expressions obtained with the BK perturbation treatment and the nuclear relaxation approach,[29,30] the latter has spawned valuable new concepts and related

computational procedures. From the viewpoint of the nuclear relaxation (NR) procedure, it is natural to divide the total vibrational (hyper)polarizability into nuclear relaxation (P^{nr}) and curvature (P^{c}) contributions. P^{nr} and P^{c} arise from the change in the electronic and zero-point vibrational averaging corrections caused by the field-induced relaxation of the equilibrium geometry, respectively. The P^{c} is usually smaller and far more computationally expensive than P^{nr},[31,32] and it is not computed here.

Under the infinite optical frequency (IOF) approximation, which corresponds to the limit $\omega \rightarrow \infty$, the expression for the dynamic P^{nr} contributions to several nonlinear optical process can be obtained using the nuclear relaxation approach.[28,30] Tests of the IOF approximation have shown that it yields satisfactory results.[33,34] The bottleneck in calculating P^{nr} from analytical expressions is the number and the computational cost of the n^{th}-order derivatives with respect to normal modes, where maximum value of n changes from 1 to 3 depending of the particular NR NLO property.[30] Their number is $(3N\text{-}6)^n$ with N being the number of atoms. This problem can be circumvented by using finite field nuclear relaxations approach. But another alternative to reduce drastically the cost of the calculations that does not prevent the calculation of the NR contributions with the analytical formulas is the use of the field-induced vibrational coordinates (FICs), which are just the displacement coordinates derived from the change in the equilibrium geometry induced by a static applied field.[34–36] The FICs radically reduce the number of n^{th}-order derivatives to be evaluated. For instance, for the average value of nuclear relaxation contribution to Pockels effect, the analytical expressions containing sums over $3N$-6 normal coordinates can be reduced to formulas that involve only three FICs.

The analytical definition of the first (χ_1^{α}) and harmonic second-order ($\chi_{2,har}^{\alpha\beta}$) FICs are based on the expansion of the field-dependent displacement of the field-free normal coordinate (Q_i^F) induced by a uniform static electric field as a power series in the field (F_α).[36] Only one first order FIC is required to calculate each diagonal component of $\alpha^{nr}(0;0)$, $\beta^{nr}(0;0,0)$, $\beta^{nr}(-\omega;\omega,0)_{\omega\rightarrow\infty}$ (IOF approximation NR Pockels β), and $\gamma^{nr}(-2\omega;\omega,\omega,0)_{\omega\rightarrow\infty}$ (IOF approximation NR field induced second harmonic (FISH) γ) tensors. And using only the three first order FICs the average value of these four NR NLO properties can be calculated. Also one unique FIC, but now the harmonic second order FIC, is necessary to calculate each diagonal component of $\gamma_{aaaa}^{nr}(-\omega;\omega,-\omega,\omega)_{\omega\rightarrow\infty}$ (IOF approximation NR intensity dependent refractive index (IDRI) γ) (the six harmonic second order FICs are required for the calculation of $\bar{\gamma}^{nr}(-\omega;\omega,-\omega,\omega)_{\omega\rightarrow\infty}$ average value). Using only two FICs, a first order and a harmonic second order FICs, one can also obtain each diagonal component of $\gamma_{aaaa}^{nr}(-\omega;\omega,0,0)_{\omega\rightarrow\infty}$ (IOF approximation NR Kerr effect γ) (the three first order FICs and the six harmonic second order FICs are necessary to obtain $\bar{\gamma}^{nr}(-\omega;\omega,0,0)_{\omega\rightarrow\infty}$) The calculation of $\gamma^{nr}(0;0,0,0)$ requires second order FICs instead of harmonic second order FICs. The calculation of second order FICs is very expensive and then the static NR second hyperpolarizabilities have not been calculated here. In terms of BK bracket[26] the nuclear relaxation contributions are given by

$$\alpha^{nr}(0;0) = [\mu^2]_1^0, \tag{4}$$

$$\beta^{nr}(0;0,0) = [\mu\alpha]_2^0 + [\mu^3]_2^I, \tag{5}$$

$$\beta^{nr}(-\omega;\omega,0)_{\omega\rightarrow\infty} = [\mu\alpha]_1^0, \tag{6}$$

$$\gamma^{nr}(-\omega;\omega,0,0)_{\omega\rightarrow\infty} = [\alpha^2]_2^0 + [\mu\beta]_2^0 + [\mu^2\alpha]_2^I, \tag{7}$$

$$\gamma^{nr}(-2\omega;\omega,\omega,0)_{\omega\rightarrow\infty} = [\mu\beta]_1^0, \tag{8}$$

and

$$\gamma^{nr}(-\omega;\omega,-\omega,\omega)_{\omega\rightarrow\infty} = [\alpha^2]_{2'}^0, \tag{9}$$

where the superindex of the square bracket indicate the total order of anharmonicity of the term; the subindex is the number of external static fields involve in the definition of the property ($2'$ is a special case to indicate that there are no static fields, but there are the cancellation of signs of two optical frequencies); and the properties inside the square bracket indicate which derivatives of the electronic property contain each term.

III. RESULTS AND DISCUSSIONS

Table I shows the experimental and theoretical bond lengths of the phenylene-containing porphyrinoid ring with C_2 topology (for the numbering of the distances see Figure 2). The bond lengths have been evaluated at HF, CAM-B3LYP, and M052X levels using the 6-31G and 6-311G(d) basis sets (gas phase). Moreover, Table I also contains the maximum absolute error (MAX) and the mean absolute error (MAE), which is defined

$$MAE = \sum_{i=1}^{N} \frac{|d_i - d_{i,exp}|}{N}, \tag{10}$$

where d_i and $d_{i,\,exp}$ are the calculated and experimental bond lengths, respectively, and N is the number of bond lengths considered ($N = 23$). From the MAE values, one can easily see that the increase from 6-31G to 6-311G(d) basis sets does not improve the agreement between theoretical and x-ray crystallographic bond lengths; e.g., at CAM-B3LYP and M052X levels the MAE value using the 6-31G and 6-311G(d) basis sets is the same, 0.015. In addition, a better geometrical description of the ring is obtained with CAM-B3LYP and M052X methods than HF; e.g., using the 6-311G(d) basis set the MAE values of HF, CAM-B3LYP, and M052X treatments are 0.023, 0.015, and 0.015, respectively. This later average error is very similar to the average error obtained for our previous results for the bianthraquinodimethane modified [16] annulene.[16] Moreover, d_1, d_6, d_{20}, d_{21}, and d_{23} are the experimental distances that show a major difference with respect to the calculated results. These bond lengths are mainly located in the carbon-carbon bonds that connect the pyrrole subunits and the bonds attached to these bridges. Among them, it is worth noting the d_1 distance, which has the maximum absolute error value for all the methods displayed in Table I.

TABLE I. Selected geometrical distances of the C_2 Möbius topology of A,D-di-p-benzi[28]hexaphyrin (1.1.1.1.1.1). All quantities are in Ångstroms.

	HF		CAM-B3LYP		M052X		
Distances[a]	6-31G	6-311G(d)	6-31G	6-311G(d)	6-31G	6-311G(d)	Expt.[b]
d_1	1.359	1.354	1.381	1.375	1.383	1.378	1.434
d_2	1.469	1.469	1.460	1.456	1.461	1.458	1.453
d_3	1.335	1.327	1.352	1.343	1.355	1.347	1.336
d_4	1.472	1.471	1.465	1.459	1.465	1.459	1.455
d_5	1.400	1.391	1.400	1.390	1.395	1.385	1.395
d_6	1.379	1.370	1.382	1.371	1.379	1.368	1.338
d_7	1.345	1.340	1.363	1.356	1.364	1.358	1.351
d_8	1.490	1.493	1.479	1.477	1.475	1.473	1.483
d_9	1.400	1.397	1.409	1.402	1.409	1.403	1.393
d_{10}	1.377	1.375	1.381	1.376	1.382	1.378	1.381
d_{11}	1.393	1.391	1.398	1.392	1.398	1.393	1.405
d_{12}	1.396	1.392	1.405	1.400	1.406	1.401	1.404
d_{13}	1.383	1.381	1.386	1.381	1.386	1.382	1.370
d_{14}	1.399	1.395	1.409	1.402	1.410	1.402	1.414
d_{15}	1.397	1.394	1.406	1.400	1.407	1.405	1.404
d_{16}	1.485	1.489	1.471	1.471	1.467	1.466	1.457
d_{17}	1.347	1.342	1.365	1.359	1.365	1.362	1.378
d_{18}	1.471	1.470	1.467	1.462	1.468	1.463	1.447
d_{19}	1.341	1.332	1.354	1.345	1.357	1.349	1.342
d_{20}	1.477	1.479	1.472	1.469	1.475	1.472	1.439
d_{21}	1.305	1.286	1.336	1.316	1.335	1.317	1.358
d_{22}	1.410	1.398	1.406	1.391	1.401	1.385	1.400
d_{23}	1.450	1.460	1.436	1.440	1.434	1.438	1.411
MAE	0.020	0.023	0.015	0.015	0.015	0.015	
MAX	0.075	0.080	0.053	0.059	0.051	0.056	

[a]For the numbering of the distances, see Figure 2.
[b]The experimental distances are obtained from the x-ray crystal structure, see Ref. 5.

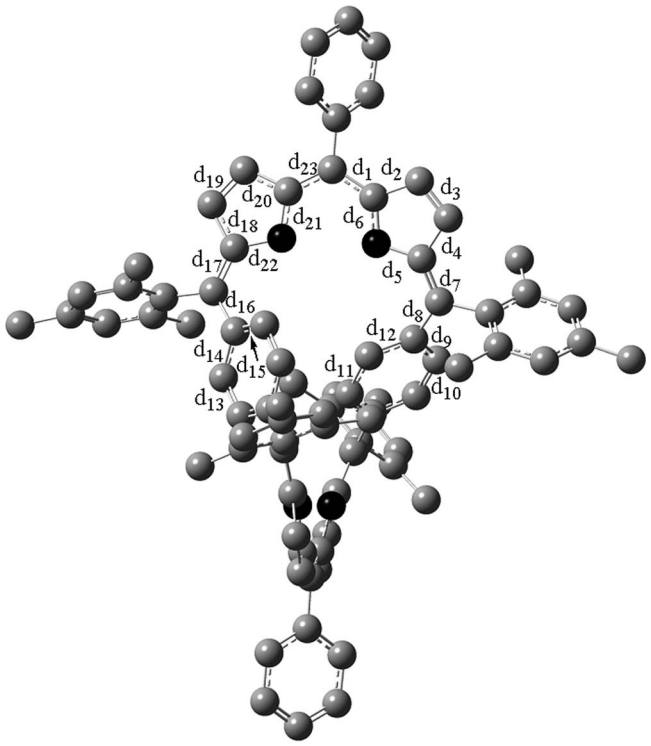

FIG. 2. Representation of the C_2 Möbius topology of A,D-di-p-benzi[28]hexaphyrin(1.1.1.1.1.1). The labels are used for the bond distances displayed in Table I. The hydrogen atoms have been omitted for clarity.

Tables II and III contain the static electronic contribution to α and γ for the structures **1-H** and **1-M**, respectively, using seven different levels of theory. For each property, the diagonal components and the average values, see Eqs. (1)–(3), are reported. The μ and β of these two conformations are very small, e.g., **1-H** has two diagonal terms null by symmetry, and no relevant conclusions can be obtained. For this reason, our analysis will be focus on α and γ values. But our results for the electronic and nuclear relaxation contributions to dipole moments and first hyperpolarizabilities of **1-H** and **1-M** can be found in the Tables S1 and S2 of the supplementary material, respectively.[37]

It is well established that diffuse and polarization functions are required for a quantitative description of both the electronic and vibrational (hyper)polarizabilities of medium size organic molecules.[32,38–41] Nevertheless, it has also been found in the past that the 6-31G basis set is adequate to obtain qualitative results, and many previous theoretical investigations of NLOP have used it.[31,36,39,40,42] In Tables II and III, one can see that the increment of basis set from 6-31G to 6-311G(d) does not provoke a large variation of α^e and γ^e values (lie in the 2%–32% range).

In our previous article,[16] we used the 6-31+G(d) basis for the NLOP evaluation of bianthraquinodimethane modified [16] annulene. In the present work, the inclusion of the diffuse functions produces a problem in the convergence of the self-consistent field (SCF) process. Then, to check the

TABLE II. Electronic polarizabilities and second hyperpolarizabilities of the Hückel topology of A,D-di-p-benzi[28]hexaphyrin(1.1.1.1.1.1) (**1-H**) calculated using 7 different levels of theory. All quantities are in atomic units.

	HF		CAM-B3LYP			M052X	
Properties	6-31G	6-311G(d)	6-31G	6-311G(d)	6-31+G(d)[a]	6-31G	6-311G(d)
$\alpha^e_{xx}(0;0)$	1.13×10^3	1.15×10^3	1.32×10^3	1.34×10^3	1.38×10^3	1.36×10^3	1.38×10^3
$\alpha^e_{yy}(0;0)$	9.27×10^2	9.73×10^2	9.56×10^2	1.04×10^3	1.08×10^3	8.88×10^2	9.89×10^2
$\alpha^e_{zz}(0;0)$	8.54×10^2	9.01×10^2	9.58×10^2	1.00×10^3	1.05×10^3	9.76×10^2	1.02×10^3
$\bar{\alpha}^e(0;0)$	9.72×10^2	1.01×10^3	1.08×10^3	1.13×10^3	1.17×10^3	1.07×10^3	1.13×10^3
$\gamma^e_{xxxx}(0;0,0,0)$	1.05×10^6	9.05×10^5	4.01×10^6	3.46×10^6	3.81×10^6	4.80×10^6	4.06×10^6
$\gamma^e_{yyyy}(0;0,0,0)$	3.29×10^5	3.07×10^5	4.45×10^5	5.68×10^5	6.64×10^5	3.26×10^5	4.28×10^5
$\gamma^e_{zzzz}(0;0,0,0)$	1.84×10^5	1.64×10^5	5.38×10^5	4.84×10^5	5.88×10^5	6.15×10^5	5.58×10^5
$\bar{\gamma}^e(0;0,0,0)$	4.30×10^5	3.82×10^5	1.27×10^6	1.18×10^6	1.34×10^6	1.38×10^6	1.29×10^6

[a]NLOP evaluated using a small SCF convergence (1×10^{-6}) at the optimized geometry at CAM-B3LYP/6-311G(d) level.

effect of the diffuse functions we have evaluated the NLOP of **1-H** and **1-M** at CAM-B3LYP/6-31+G(d) level using a low SCF convergence (1.0×10^{-6}) at the optimized geometry obtained at CAM-B3LYP/6-311G(d). In Tables II and III, we can see that the diffuse functions have also an small effect in the electronic contribution and they only imply a small augment of the values obtained with the 6-311G(d) basis set; i.e., less than 5% and 15% for $\bar{\alpha}^e$ and $\bar{\gamma}^e$, respectively. On the other hand, the electronic correlation results essential for the correct evaluation of NLOP. The CAM-B3LYP and M052X methodologies increase $\bar{\alpha}^e$ values around 10% with respect to the HF level, while $\bar{\gamma}^e$ values for the Hückel and Möbius topologies are increased around 200% and 300%, respectively. It is worth noting the case of $\bar{\gamma}^e$ at the Möbius topology, which shows the values of 3.84×10^5 and 1.65×10^6 at the HF/6-311G(d) and M052X/6-311G(d) methods, respectively. But CAM-B3LYP and M052X methods show very similar $\bar{\alpha}^e$ and $\bar{\gamma}^e$ values (differences lie in the range 1%–13%). Then, we can conclude that CAM-B3LYP/6-31G and M052X/6-31G levels can provide a semiquantitative accuracy to evaluate the electronic NLOP of expanded porphyrins.

In Tables II and III one can check that the Möbius and Hückel conformations show very similar values for $\bar{\alpha}^e$. But in contrast to our previous article,[16] the Möbius $\bar{\gamma}^e$ values are larger than the Hückel $\bar{\gamma}^e$ for all the quantum chemistry methods studied in this work. However, this difference is not relevant enough to consider this system as an efficient topological switch at gas phase, *i.e.* the largest difference of $\bar{\gamma}^e_{\text{Möbius}}/\bar{\gamma}^e_{\text{Hückel}}$ is 1.35 at M052X/6-31G level.

Stepień *et al.*[5] show that the equilibrium between Hückel and Möbius conformers of A,D-di-p-benzi[28]hexaphyrin(1.1.1.1.1.1) is solvent-dependent. Then, we have also checked the role of the solvent in the evaluation of the NLOP, optimizing the **1-H** and **1-M** structures using the SCRF approach with a dielectric constant of benzene ($\varepsilon = 2.271$), chloroform ($\varepsilon = 4.711$), and ethanol ($\varepsilon = 24.852$) at CAM-B3LYP/6-31G level, see Table IV. One can easily see that α^e and γ^e values increase with the dielectric constant of the solvent.[37] For instance, at the Möbius conformation $\bar{\gamma}^e$ evaluated at benzene, chloroform, and ethanol solvents is 2.2, 3.5, and 4.9 times, respectively, larger than $\bar{\gamma}^e$ evaluated at gas phase. However, the ratio $\bar{\gamma}^e_{\text{Möbius}}/\bar{\gamma}^e_{\text{Hückel}}$ with solvent remains more or less constant than the results obtained with gas phase. The difference of the NLOP between the Möbius and Hückel structures also increases with the dielectric constant, e.g., the difference of $\bar{\gamma}^e$ evaluated of gas phase and benzene, chloroform, and ethanol solvents are 3.57×10^5, 6.49×10^5, 1.04×10^6, and 1.26×10^6, respectively. These results indicate that the solvent has a relevant role in the evaluation of the NLOP. And then, it is necessary to consider explicit solvent molecules to a correct study of the NLOP for expanded porphyrins, although this fact is out of the scope of the present work.

TABLE III. Electronic polarizabilities and second hyperpolarizabilities of Möbius topology of A,D-di-p-benzi[28]hexaphyrin(1.1.1.1.1.1) (**1-M**) calculated using 7 different levels of theory. All quantities are in atomic units.

	HF		CAM-B3LYP			M052X	
Properties	6-31G	6-311G(d)	6-31G	6-311G(d)	6-31+G(d)[a]	6-31G	6-311G(d)
$\alpha^e_{xx}(0;0)$	1.12×10^3	1.15×10^3	1.31×10^3	1.33×10^3	1.38×10^3	1.32×10^3	1.36×10^3
$\alpha^e_{yy}(0;0)$	9.90×10^2	1.02×10^3	1.06×10^3	1.12×10^3	1.16×10^3	1.04×10^3	1.10×10^3
$\alpha^e_{zz}(0;0)$	8.07×10^2	8.60×10^2	8.95×10^2	9.50×10^2	9.97×10^2	9.01×10^2	9.67×10^2
$\bar{\alpha}^e(0;0)$	9.73×10^2	1.01×10^3	1.09×10^3	1.14×10^3	1.18×10^3	1.09×10^3	1.14×10^3
$\gamma^e_{xxxx}(0;0,0,0)$	1.03×10^6	8.66×10^5	5.32×10^6	4.44×10^6	4.79×10^6	6.32×10^6	5.28×10^6
$\gamma^e_{yyyy}(0;0,0,0)$	3.77×10^5	3.27×10^5	6.30×10^5	6.89×10^5	7.91×10^5	6.47×10^5	6.73×10^5
$\gamma^e_{zzzz}(0;0,0,0)$	1.74×10^5	1.59×10^5	4.30×10^5	4.16×10^5	5.15×10^5	4.80×10^5	4.89×10^5
$\bar{\gamma}^e(0;0,0,0)$	4.41×10^5	3.84×10^5	1.62×10^6	1.45×10^6	1.61×10^6	1.87×10^6	1.65×10^6

[a]NLOP evaluated using a small SCF convergence (1×10^{-6}) at the optimized geometry at CAM-B3LYP/6-311G(d) level.

TABLE IV. CAM-B3LYP/6-31G electronic polarizabilities and second hyperpolarizabilities of Hückel and Möbius topologies of A,D-di-p-benzi[28]hexaphyrin(1.1.1.1.1.1) calculated at gas phase and three different solvents (PCM-SMD solvation model). All quantities are in atomic units.

Properties	Gas phase	Benzene	Chloroform	Ethanol
Hückel (**1-H**)				
$\alpha^e_{xx}(0;0)$	1.32×10^3	1.62×10^3	1.79×10^3	1.96×10^3
$\alpha^e_{yy}(0;0)$	9.56×10^2	1.21×10^3	1.36×10^3	1.50×10^3
$\alpha^e_{zz}(0;0)$	9.58×10^2	1.17×10^3	1.27×10^3	1.38×10^3
$\bar{\alpha}^e(0;0)$	1.08×10^3	1.33×10^3	1.47×10^3	1.62×10^3
$\gamma^e_{xxxx}(0;0,0,0)$	4.01×10^6	8.87×10^6	1.30×10^7	1.86×10^7
$\gamma^e_{yyyy}(0;0,0,0)$	4.45×10^5	1.18×10^6	1.84×10^6	2.64×10^6
$\gamma^e_{zzzz}(0;0,0,0)$	5.38×10^5	1.13×10^6	1.53×10^6	2.21×10^6
$\bar{\gamma}^e(0;0,0,0)$	1.27×10^6	2.86×10^6	4.23×10^6	6.17×10^6
Möbius (**1-M**)				
$\alpha^e_{xx}(0;0)$	1.31×10^3	1.59×10^3	1.76×10^3	1.92×10^3
$\alpha^e_{yy}(0;0)$	1.06×10^3	1.32×10^3	1.48×10^3	1.61×10^3
$\alpha^e_{zz}(0;0)$	8.95×10^2	1.08×10^3	1.19×10^3	1.30×10^3
$\bar{\alpha}^e(0;0)$	1.09×10^3	1.33×10^3	1.48×10^3	1.61×10^3
$\gamma^e_{xxxx}(0;0,0,0)$	5.32×10^6	1.13×10^7	1.67×10^7	2.34×10^7
$\gamma^e_{yyyy}(0;0,0,0)$	6.30×10^5	1.46×10^6	2.30×10^6	3.40×10^6
$\gamma^e_{zzzz}(0;0,0,0)$	4.30×10^5	8.88×10^5	1.30×10^6	1.84×10^6
$\bar{\gamma}^e(0;0,0,0)$	1.62×10^6	3.51×10^6	5.26×10^6	7.43×10^6

Tables V and VI report the static and IOF dynamic nuclear relaxation polarizabilities and second hyperpolarizabilities for **1-H** and **1-M** structures, respectively. The evaluation of the three diagonal components of $\gamma^{nr}(-\omega;\ \omega,\ 0,\ 0)_{\omega\to\infty}$ and $\gamma^{nr}(-2\omega;\ \omega,\ \omega,\ 0)_{\omega\to\infty}$ properties are computational expensive (they require 13 Hessian calculations) and for the largest basis set, 6-311G(d), they have been only evaluated at CAM-B3LYP level. On the other hand, other properties such as $\alpha^{nr}(0;\ 0)$ and $\gamma^{nr}(-\omega;\ \omega,\ -\omega,\ \omega)_{\omega\to\infty}$ only require the Hessian calculation at the equilibrium geometry and they have been evaluated for all the quantum chemistry methods studied in this work, in exception of the M052X/6-311G(d) level, where the high accurate optimized geometries requested for the evaluation of the nuclear relaxation linear polarizabilities and second hyperpolarizabilities was not achieved. In analogy to our previous work,[16] the vibrational contribution to static and IOF dynamic NLOP can be either larger or comparable in size than the electronic contribution. For instance, in the Hückel conformer $\bar{\gamma}^{nr}(-\omega;\omega,0,0)_{\omega\to\infty}$ and $\bar{\gamma}^{nr}(-\omega;\omega,-\omega,\omega)_{\omega\to\infty}$ evaluated at CAM-B3LYP/6-311G(d) are 1.2 and 2.3 larger than $\bar{\gamma}^e(0;0,0,0)$. Then, it results than an accurate evaluation of NLOP for expanded porphyrins requires the study of the vibrational contribution.

In contrast to the electronic contribution, the modifications of the basis set and/or method provoke important differences in the independent components of the nuclear relaxation α and γ tensors. However, the big differences are largely cancelled in the average nuclear relaxation values of α and γ. The increment of basis set from 6-31G to 6-311G(d) does not provoke large variations of $\bar{\alpha}^{nr}$ and $\bar{\gamma}^{nr}$, which differences lie in the range 1%–17%, with one relevant exception, $\bar{\gamma}^{nr}(-\omega;\omega,0,0)_{\omega\to\infty}$ at CAM-B3LYP in the **1-M** structure. The latter is caused only by the basis set dependence of the BK $[\mu^2\alpha]^I_2$ term, which is an indication that the anharmonicity plays a crucial role in this property for this system. On the other hand, the density functional theory methods induce important modifications

TABLE V. Nuclear relaxation polarizabilities and second hyperpolarizabilities of Hückel topology of A,D-di-p-benzi[28]hexaphyrin(1.1.1.1.1.1) (**1-H**) calculated using 5 different levels of theory. All quantities are in atomic units.

	HF		CAM-B3LYP		M052X
Properties	6-31G	6-311G(d)[a]	6-31G	6-311G(d)	6-31G
$\alpha^{nr}_{xx}(0;0)$	1.00×10^2	9.28×10^1	8.83×10^1	1.25×10^2	9.01×10^1
$\alpha^{nr}_{yy}(0;0)$	9.89×10^1	1.01×10^2	9.98×10^1	1.09×10^2	9.62×10^1
$\alpha^{nr}_{zz}(0;0)$	7.20×10^1	6.49×10^1	6.86×10^1	7.39×10^1	5.99×10^1
$\bar{\alpha}^{nr}(0;0)$	9.04×10^1	8.64×10^1	8.56×10^1	1.02×10^2	8.21×10^1
$\gamma^{nr}_{xxxx}(-\omega;\omega,0,0)_{\omega\to\infty}$	9.74×10^5		2.65×10^6	-2.81×10^5	2.93×10^6
$\gamma^{nr}_{yyyy}(-\omega;\omega,0,0)_{\omega\to\infty}$	6.56×10^5		1.54×10^6	1.60×10^6	-5.13×10^5
$\gamma^{nr}_{zzzz}(-\omega;\omega,0,0)_{\omega\to\infty}$	4.43×10^5		7.28×10^5	7.58×10^5	7.17×10^5
$\bar{\gamma}^{nr}(-\omega;\omega,0,0)_{\omega\to\infty}$[b,c]	7.46×10^5		1.25×10^6	1.41×10^6	9.73×10^5
$\gamma^{nr}_{xxxx}(-2\omega;\omega,\omega,0)_{\omega\to\infty}$	6.09×10^4		2.16×10^5	1.55×10^5	2.46×10^5
$\gamma^{nr}_{yyyy}(-2\omega;\omega,\omega,0)_{\omega\to\infty}$	-1.17×10^4		-3.92×10^4	-2.46×10^4	-1.68×10^4
$\gamma^{nr}_{zzzz}(-2\omega;\omega,\omega,0)_{\omega\to\infty}$	2.92×10^3		-9.86×10^3	-5.18×10^3	-1.28×10^4
$\bar{\gamma}^{nr}(-2\omega;\omega,\omega,0)_{\omega\to\infty}$	-2.23×10^4		-4.69×10^4	-4.47×10^4	-3.70×10^4
$\gamma^{nr}_{xxxx}(-\omega;\omega,-\omega,\omega)_{\omega\to\infty}$	1.94×10^6	1.80×10^6	4.21×10^6	4.20×10^6	4.22×10^6
$\gamma^{nr}_{yyyy}(-\omega;\omega,-\omega,\omega)_{\omega\to\infty}$	1.73×10^6	1.65×10^6	2.91×10^6	3.28×10^6	1.55×10^6
$\gamma^{nr}_{zzzz}(-\omega;\omega,-\omega,\omega)_{\omega\to\infty}$	7.16×10^5	6.72×10^5	1.59×10^6	1.47×10^6	1.32×10^6
$\bar{\gamma}^{nr}(-\omega;\omega,-\omega,\omega)_{\omega\to\infty}$[b]	1.48×10^6	1.39×10^6	2.56×10^6	2.68×10^6	2.25×10^6

[a] $\gamma^{nr}(-\omega;\omega,0,0)_{\omega\to\infty}$ and $\gamma^{nr}(-2\omega;\omega,\omega,0)_{\omega\to\infty}$ properties at HF/6-311G(d) level have not been evaluated for computational limitations.

[b] The $[\alpha^2]$ terms were calculated using the 3*N*-6 normal modes.

[c] The $[\mu^2\alpha]$ terms of $\gamma^{nr}_{abba}(-\omega;\omega,0,0)_{\omega\to\infty}$ non-diagonal components are approximate. The exact calculation of such square bracket terms requires using the three non-diagonal $\chi^{xy}_{2,har}$, $\chi^{xz}_{2,har}$, and $\chi^{yz}_{2,har}$ second-order FICs as well as the six diagonal first-order and harmonic second-order FICs used here (see Table I of Ref. 36 for more details).

TABLE VI. Nuclear relaxation polarizabilities and second hyperpolarizabilities of Möbius topology of A,D-di-p-benzi[28]hexaphyrin(1.1.1.1.1.1) (**1-M**) calculated using 5 different levels of theory. All quantities are in atomic units.

	HF		CAM-B3LYP		M052X
Properties	6-31G	6-311G(d)[a]	6-31G	6-311G(d)	6-31G
$\alpha^{nr}_{xx}(0;0)$	9.39×10^1	9.07×10^1	9.19×10^1	1.11×10^2	7.91×10^1
$\alpha^{nr}_{yy}(0;0)$	9.99×10^1	1.02×10^2	9.73×10^1	9.54×10^1	8.44×10^1
$\alpha^{nr}_{zz}(0;0)$	7.78×10^1	7.02×10^1	8.10×10^1	7.33×10^1	6.79×10^1
$\bar{\alpha}^{nr}(0;0)$	9.05×10^1	8.75×10^1	9.01×10^1	9.32×10^1	7.71×10^1
$\gamma^{nr}_{xxxx}(-\omega;\omega,0,0)_{\omega\to\infty}$	8.78×10^5		2.23×10^6	2.19×10^6	3.07×10^6
$\gamma^{nr}_{yyyy}(-\omega;\omega,0,0)_{\omega\to\infty}$	9.73×10^5		-3.81×10^6	6.73×10^5	1.64×10^6
$\gamma^{nr}_{zzzz}(-\omega;\omega,0,0)_{\omega\to\infty}$	4.14×10^5		7.29×10^6	5.72×10^5	5.52×10^5
$\bar{\gamma}^{nr}(-\omega;\omega,0,0)_{\omega\to\infty}$[b,c]	6.44×10^5		2.59×10^5	1.33×10^6	1.52×10^6
$\gamma^{nr}_{xxxx}(-2\omega;\omega,\omega,0)_{\omega\to\infty}$	5.29×10^4		2.86×10^4	2.90×10^4	4.56×10^3
$\gamma^{nr}_{yyyy}(-2\omega;\omega,\omega,0)_{\omega\to\infty}$	-5.28×10^3		-4.98×10^4	-4.61×10^4	-1.22×10^4
$\gamma^{nr}_{zzzz}(-2\omega;\omega,\omega,0)_{\omega\to\infty}$	3.30×10^3		-1.94×10^4	-1.51×10^4	-3.76×10^4
$\bar{\gamma}^{nr}(-2\omega;\omega,\omega,0)_{\omega\to\infty}$	-2.33×10^4		-9.35×10^4	-8.77×10^4	-8.67×10^4
$\gamma^{nr}_{xxxx}(-\omega;\omega,-\omega,\omega)_{\omega\to\infty}$	1.72×10^6	1.59×10^6	4.99×10^6	4.69×10^6	5.53×10^6
$\gamma^{nr}_{yyyy}(-\omega;\omega,-\omega,\omega)_{\omega\to\infty}$	1.83×10^6	1.78×10^6	2.73×10^6	3.09×10^6	1.83×10^6
$\gamma^{nr}_{zzzz}(-\omega;\omega,-\omega,\omega)_{\omega\to\infty}$	9.29×10^5	8.50×10^5	1.75×10^6	1.69×10^6	1.42×10^6
$\bar{\gamma}^{nr}(-\omega;\omega,-\omega,\omega)_{\omega\to\infty}$[b]	1.57×10^6	1.47×10^6	2.93×10^6	2.95×10^6	2.85×10^6

[a] $\gamma^{nr}(-\omega;\omega,0,0)_{\omega\to\infty}$ and $\gamma^{nr}(-2\omega;\omega,\omega,0)_{\omega\to\infty}$ properties at HF/6-311G(d) level have not been evaluated for computational limitations.

[b] The $[\alpha^2]$ terms were calculated using the $3N$-6 normal modes.

[c] The $[\mu^2\alpha]$ terms of $\gamma^{nr}_{abba}(-\omega;\omega,0,0)_{\omega\to\infty}$ non-diagonal components are approximate. The exact calculation of such square bracket terms requires using the three non-diagonal $\chi^{xy}_{2,har}$, $\chi^{xz}_{2,har}$, and $\chi^{yz}_{2,har}$ second-order FICs as well as the six diagonal first-order and harmonic second-order FICs used here (see Table I of Ref. 36 for more details).

of the average nuclear relaxation values of α and γ, i.e., $\bar{\alpha}^{nr}$ and $\bar{\gamma}^{nr}$ evaluated using the CAM-B3LYP and M052X methodologies vary from 23% to 150% in comparison with the results obtained at HF level. These differences are reduced (smaller than 33%) comparing the $\bar{\alpha}^{nr}$ and $\bar{\gamma}^{nr}$ results obtained with CAM-B3LYP and M052X methods, although an exception is obtained with the $\bar{\gamma}^{nr}(-\omega;\omega,0,0)_{\omega\to\infty}$ at the Möbius conformer, which presents the values of 2.59×10^5 and 1.52×10^6 using the CAM-B3LYP/6-31G and M052X/6-31G levels, respectively. Then, we can conclude that CAM-B3LYP/6-31G and M052X/6-31G methods can provide at least a qualitative description of the vibrational contribution for the NLOP of expanded porphyrins.

In a similar way to the electronic contribution, the Möbius conformation shows larger $\bar{\gamma}^{nr}$ values (for most of properties) than the Hückel structure. For instance, at M052X/6-31G level we obtain that the ratios of $\bar{\gamma}^{nr}(-\omega;\omega,0,0)_{\omega\to\infty}$, $\bar{\gamma}^{nr}(-2\omega;\omega,\omega,0)_{\omega\to\infty}$, and $\bar{\gamma}^{nr}(-\omega;\omega,-\omega,\omega)_{\omega\to\infty}$ of the Möbius structure with respect to the Hückel conformer are 1.6, 2.3, and 1.3, respectively. Thus, to reproduce the possible experimental results it is necessary to consider the sum of the static electronic and vibrational contributions ($\bar{\gamma} = \bar{\gamma}^e + \bar{\gamma}^{vib}$), which shows very high values (lie in the range 4×10^5 and 5×10^6 a.u.). In the literature, several works have shown that second hyperpolarizabilites larger than 1×10^5 a.u. can be considered as high NLOP values.[40,41,43] For instance, the $\bar{\gamma}$ obtained in this work are one order of magnitude larger than our results obtained for the Hückel and Möbius conformers for the bianthraquinodimethane modified [16] annulene.[16] It is important to remark that large differences of $\bar{\gamma}$ between the Hückel and Möbius conformers are obtained, the maximum difference is 1×10^6 a.u. [electronic contribution plus NR Kerr effect and electronic contribution plus NR IDRI effect evaluated at M052X/6-31G]. These results are promising to manufacture Hückel-to-Möbius topological switches based on expanded porphyrins with high NLOP and large differences between the Möbius and Hückel conformations.

IV. SUMMARY AND CONCLUSIONS

With the aim of bringing more insight into the relationship between aromaticity, molecular geometry, and NLOP for the expanded porphyrins, we have evaluated the electronic and vibrational contributions to static and IOF dynamic NLOP of the Hückel and Möbius conformers of A,D-di-p-benzi[28]hexaphyrin(1.1.1.1.1.1) synthesized by Latos-Grażyński and co-workers. Calculations are performed at the HF, M052X, and CAM-B3LYP levels using the 6-31G, 6-311G(d), and 6-31+G(d) basis sets in gas phase. Moreover, the solvation effect in the electronic contribution to NLOP has also been considered using the PCM-SMD approach with three different solvents (benzene, chloroform, and ethanol) evaluated at CAM-B3LYP/6-31G methodology. The results of this work lead us to the following conclusions:

(a) CAM-B3LYP/6-31G and M052X/6-31G methods correctly reproduce the X-Ray crystal structure of the **1-M** conformer and they provide a semiquantitative accuracy to evaluate the static electronic NLOP of expanded porphyrins.

(b) The static electronic contribution to NLOP and the difference of the NLOP between the Möbius and Hückel structures increase with the dielectric constant of the solvent, although it does not change the general conclusions obtained at gas phase. These results indicate that the solvent has a relevant role in the evaluation of the NLOP and then it is necessary to consider explicit solvent molecules in their accurate calculation.

(c) In expanded porphyrins, the vibrational contribution to static and IOF dynamic NLOP can be either larger or comparable in size than the electronic contribution and it must to be considered for an accurate evaluation of NLOP. Moreover, the modifications of the basis set and/or method provoke important differences in the nuclear relaxation of α and γ. However, we found that CAM-B3LYP/6-31G and M052X/6-31G levels can provide at least a qualitative description of the vibrational contribution for the NLOP of expanded porphyrins.

(d) The sum of the electronic and vibrational contributions, $\bar{\gamma}$, shows very high values (lie in the range 4×10^5 and 5×10^6 a.u.) and large differences of $\bar{\gamma}$ between the Hückel and Möbius conformers are obtained, with the maximum difference at 1×10^6 a.u.

These results are promising for the design and photophysical characterization of new Hückel-to-Möbius topological switches based on expanded porphyrins. It is worth noting that in gas phase the Hückel conformer of A,D-di-p-benzi[28]hexaphyrin(1.1.1.1.1.1) is more stable than the Möbius structure, i.e., the aromaticity plays a small role in the relative stability of this switch. We expect that higher NLOP values and larger differences between NLOP of Möbius and Hückel conformations can be obtained in expanded porphyrins with larger differences of aromaticity (and HOMO-LUMO gaps) between both topologies, and where the Möbius structure is most stable than the Hückel one. Additional work on the NLOP evaluation of meso-aryl-substituted [28]hexaphyrins(1.1.1.1.1.1),[8] and a deep analysis between the aromaticity, global hardness, and NLOP of the expanded porphyrins using the maximum hardness and minimum polarizability principles[44] are in progress in our laboratory.

ACKNOWLEDGMENTS

This research has been supported by the Spanish Dirección General de Investigación Científica y Técnica (DGYCIT, Grant Nos. CTQ2011-27812/BQU and CTQ2011-23156/BQU), the Generalitat de Catalunya (Grant Nos. 2009SGR01472 and 2009SGR637), and the Research Executive Agency (Grant Agreement No. PERG05-GA-2009-249310). The calculations described in this work were carried out at the Centre de Supercomputació de Catalunya (CESCA). M.T-S. acknowledges the CSIC for the JAE-DOC contract.

[1] E. Heilbronner, Tetrahedron Lett. **5**, 1923 (1964); H. E. Zimmerman, J. Am. Chem. Soc. **88**, 1564 (1966); M. Mauksch, V. Gogonea, H. Jiao, and P. v. R. Schleyer, Angew. Chem., Int. Ed. **37**, 2395 (1998); H. S. Rzepa, Chem. Rev. **105**, 3697 (2005); C. Castro, Z. F. Chen, C. S. Wannere, H. J. Jiao, W. L. Karney, M. Mauksch, R. Puchta, N. Hommes, and P. v. R. Schleyer, J. Am. Chem. Soc. **127**, 2425 (2005); C. Castro, W. L. Karney, M. A. Valencia, C. M. H. Vu, and R. P. Pemberton, *ibid.* **127**, 9704 (2005); D. Ajami, K. Hess, F. Kohler, C. Nather, O. Oeckler, A. Simon, C. Yamamoto, Y. Okamoto, and R. Herges, Chem.-Eur. J. **12**, 5434 (2006); C. S. M. Allan and H. S. Rzepa, J. Chem. Theory Comput. **4**, 1841 (2008); S. M. Rappaport and H. S. Rzepa, J. Am. Chem. Soc. **130**, 7613 (2008); H. S. Rzepa, Inorg. Chem. **47**, 8932 (2008); E. W. S. Caetano, V. N. Freire, S. G. dos Santos, D. S. Galvao, and F. Sato, J. Chem. Phys. **128**, 164719 (2008); E. W. S. Caetano, V. N. Freire, S. G. dos Santos, E. L. Albuquerque, D. S. Galvao, and F. Sato, Langmuir **25**, 4751 (2009); G. Bucher, S. Grimme, R. Huenerbein, A. A. Auer, E. Mucke, F. Kohler, J. Siegwarth, and R. Herges, Angew. Chem., Int. Ed. **48**, 9971 (2009); M. Mauksch and S. B. Tsogoeva, *ibid.* **48**, 2959 (2009); Chem.-Eur. J. **16**, 7843 (2010); A. R. Mohebbi, E. K. Mucke, G. R. Schaller, F. Kohler, F. D. Sonnichsen, L. Ernst, C. Nather, and R. Herges, *ibid.* **16**, 7767 (2010); H. Fliegl, D. Sundholm, and F. Pichierri, Phys. Chem. Chem. Phys. **13**, 20659 (2011); E. Pacholska-Dudziak, L. Szterenberg, and L. Latos-Grażyński, Chem.-Eur. J. **17**, 3500 (2011).

[2] D. Ajami, O. Oeckler, A. Simon, and R. Herges, Nature (London) **426**, 819 (2003).

[3] J. L. Sessler and D. Seidel, Angew. Chem., Int. Ed. **42**, 5134 (2003).

[4] N. Jux, Angew. Chem., Int. Ed. **47**, 2543 (2008); Z. S. Yoon, A. Osuka, and D. Kim, Nat. Chem. **1**, 113 (2009); J. Y. Shin, K. S. Kim, M. C. Yoon, J. M. Lim, Z. S. Yoon, A. Osuka, and D. Kim, Chem. Soc. Rev. **39**, 2751 (2010); S. Saito and A. Osuka, Angew. Chem., Int. Ed. **50**, 4342 (2011); M. Stepień, N. Sprutta, and L. Latos-Grażyński, *ibid.* **50**, 4288 (2011).

[5] M. Stepień, L. Latos-Grażyński, N. Sprutta, P. Chwalisz, and L. Szterenberg, Angew. Chem., Int. Ed. **46**, 7869 (2007).

[6] S. Saito, J. Y. Shin, J. M. Lim, K. S. Kim, D. Kim, and A. Osuka, Angew. Chem., Int. Ed. **47**, 9657 (2008); J. Y. Shin, J. M. Lim, Z. S. Yoon, K. S. Kim, M. C. Yoon, S. Hiroto, H. Shinokubo, S. Shimizu, A. Osuka, and D. Kim, J. Phys. Chem. B **113**, 5794 (2009); T. Koide, K. Youfu, S. Saito, and A. Osuka, Chem. Commun. 6047 (2009); J. M. Lim, J. Y. Shin, Y. Tanaka, S. Saito, A. Osuka, and D. Kim, J. Am. Chem. Soc. **132**, 3105 (2010); M. C. Yoon, J. Y. Shin, J. M. Lim, S. Saito, T. Yoneda, A. Osuka, and D. Kim, Chem.-Eur. J. **17**, 6707 (2011).

[7] M. Stepień, B. Szyszko, and L. Latos-Grażyński, J. Am. Chem. Soc. **132**, 3140 (2010).

[8] J. Sankar, S. Mori, S. Saito, H. Rath, M. Suzuki, Y. Inokuma, H. Shinokubo, K. S. Kim, Z. S. Yoon, J. Y. Shin, J. M. Lim, Y. Matsuzaki, O. Matsushita, A. Muranaka, N. Kobayashi, D. Kim, and A. Osuka, J. Am. Chem. Soc. **130**, 13568 (2008).

[9] K. S. Kim, Z. S. Yoon, A. B. Ricks, J. Y. Shin, S. Mori, J. Sankar, S. Saito, Y. M. Jung, M. R. Wasielewski, A. Osuka, and D. Kim, J. Phys. Chem. A **113**, 4498 (2009); M. C. Yoon, P. Kim, H. Yoo, S. Shimizu, T. Koide, S. Tokuji, S. Saito, A. Osuka, and D. Kim, J. Phys. Chem. B **115**, 14928 (2011).

[10] Y. Tanaka, S. Saito, S. Mori, N. Aratani, H. Shinokubo, N. Shibata, Y. Higuchi, Z. S. Yoon, K. S. Kim, S. B. Noh, J. K. Park, D. Kim, and A. Osuka, Angew. Chem., Int. Ed. **47**, 681 (2008); J. K. Park, Z. S. Yoon, M. C. Yoon, K. S. Kim, S. Mori, J. Y. Shin, A. Osuka, and D. Kim, J. Am. Chem. Soc. **130**, 1824 (2008); T. Tanaka, T. Sugita, S. Tokuji, S. Saito, and A. Osuka, Angew. Chem., Int. Ed. **49**, 6619 (2010); T. Higashino, M. Inoue, and A. Osuka, J. Org. Chem. **75**, 7958 (2010); M. Inoue, T. Yoneda, K. Youfu, N. Aratani, and A. Osuka, Chem.-Eur. J. **17**, 9028 (2011).

[11] M. C. Yoon, S. Cho, M. Suzuki, A. Osuka, and D. Kim, J. Am. Chem. Soc. **131**, 7360 (2009); S. Tokuji, J. Y. Shin, K. S. Kim, J. M. Lim, K. Youfu, S. Saito, D. Kim, and A. Osuka, *ibid.* **131**, 7240 (2009); M. Inoue, K. S. Kim, M. Suzuki, J. M. Lim, J. Y. Shin, D. Kim, and A. Osuka, Angew. Chem., Int. Ed. **48**, 6687 (2009).

[12] J. M. Lim, Z. S. Yoon, J. Y. Shin, K. S. Kim, M. C. Yoon, and D. Kim, Chem. Commun. 261 (2009).

[13] H. L. Xu, Z. R. Li, F. F. Wang, D. Wu, K. Harigaya, and F. L. Gu, Chem. Phys. Lett. **454**, 323 (2008); H. L. Xu, Z. R. Li, Z. M. Su, S. Muhammad, F. L. Gu, and K. Harigaya, J. Phys. Chem. C **113**, 15380 (2009).

[14] Y. F. Wang, Z. Li, Y. Li, Z. R. Li, Z. J. Li, D. Wu, F. Ma, and C. C. Sun, Phys. Chem. Chem. Phys. **12**, 8847 (2010).

[15] Y. F. Wang, Y. Wang, Z. R. Li, Z. Li, H. L. Xu, and C. C. Sun, Int. J. Quantum Chem. **111**, 2406 (2011).

[16] M. Torrent-Sucarrat, J. M. Anglada, and J. M. Luis, J. Chem. Theory Comput. **7**, 3935 (2011).

[17] Y. Zhao, N. E. Schultz, and D. G. Truhlar, J. Chem. Theory Comput. **2**, 364 (2006).

[18] T. Yanai, D. P. Tew, and N. C. Handy, Chem. Phys. Lett. **393**, 51 (2004).

[19]W. J. Hehre, R. Ditchfield, and J. A. Pople, J. Chem. Phys. **56**, 2257 (1972); W. J. Hehre, L. Radom, P. v. R. Schleyer, and J. A. Pople, *Ab Initio Molecular Orbital Theory* (Wiley, New York, 1986).
[20]M. J. Frisch, G. W. Trucks, H. B. Schlegel *et al.*, GAUSSIAN 09, Revision B.1, Gaussian, Inc., Wallingford, CT, 2009.
[21]P. J. Davis and P. Rabinowitz, in *Numerical Integration* (Blasdell, London, 1967), p. 166; B. Champagane and N. Kirtman, in *Handbook of Advanced Electronic and Photonic Materials*, edited by H. S. Nalwas (Academic, San Diego, 2001), Vol. 9, p. 63.
[22]D. M. Bishop and P. Norman, in *Handbook of Advanced Electronic and Photonic Materials*, edited by H. S. Nalwas (Academic, San Diego, 2001), Vol. 9, p. 1.
[23]J. Tomasi, B. Mennucci, and R. Cammi, Chem. Rev. **105**, 2999 (2005).
[24]A. V. Marenich, C. J. Cramer, and D. G. Truhlar, J. Phys. Chem. B **113**, 6378 (2009).
[25]D. M. Bishop and B. Kirtman, J. Chem. Phys. **95**, 2646 (1991); **97**, 5255 (1992).
[26]D. M. Bishop, J. M. Luis, and B. Kirtman, J. Chem. Phys. **108**, 10013 (1998).
[27]O. Christiansen, J. Chem. Phys. **122**, 194105 (2005); O. Christiansen, J. Kongsted, M. J. Paterson, and J. M. Luis, *ibid.* **125**, 214309 (2006).
[28]D. M. Bishop, M. Hasan, and B. Kirtman, J. Chem. Phys. **103**, 4157 (1995).
[29]J. M. Luis, M. Duran, and J. L. Andres, J. Chem. Phys. **107**, 1501 (1997); B. Kirtman, J. M. Luis, and D. M. Bishop, *ibid.* **108**, 10008 (1998).
[30]J. M. Luis, J. Marti, M. Duran, J. L. Andres, and B. Kirtman, J. Chem. Phys. **108**, 4123 (1998).
[31]M. Torrent-Sucarrat, M. Solà, M. Duran, J. M. Luis, and B. Kirtman, J. Chem. Phys. **116**, 5363 (2002).
[32]M. Torrent-Sucarrat, M. Solà, M. Duran, J. M. Luis, and B. Kirtman, J. Chem. Phys. **120**, 6346 (2004).
[33]D. M. Bishop and E. K. Dalskov, J. Chem. Phys. **104**, 1004 (1996); O. Quinet and B. Champagne, *ibid.* **109**, 10594 (1998).
[34]J. M. Luis, M. Duran, and B. Kirtman, J. Chem. Phys. **115**, 4473 (2001).
[35]J. M. Luis, M. Duran, J. L. Andres, B. Champagne, and B. Kirtman, J. Chem. Phys. **111**, 875 (1999); J. M. Luis, B. Champagne, and B. Kirtman, Int. J. Quantum Chem. **80**, 471 (2000).
[36]J. M. Luis, M. Duran, B. Champagne, and B. Kirtman, J. Chem. Phys. **113**, 5203 (2000).
[37]See supplementary material at http://dx.doi.org/10.1063/1.4765667 for Tables S1 and S2 that show the electronic and nuclear relaxation dipole moments and first hyperpolarizabilities of **1-H** and **1-M**, respectively. Table S3 displays the CAM-B3LYP/6-31G electronic dipole moments and first hyperpolarizabilities of **1-H** and **1-M** calculated at gas phase and three different solvents.
[38]M. Torrent-Sucarrat, M. Solà, M. Duran, J. M. Luis, and B. Kirtman, J. Chem. Phys. **118**, 711 (2003); K. Y. Suponitsky, S. Tafur, and A. E. Masunov, *ibid.* **129**, 044109 (2008).
[39]P. A. Limacher, K. V. Mikkelsen, and H. P. Luthi, J. Chem. Phys. **130**, 194114 (2009).
[40]H. Reis, O. Loboda, A. Avramopoulos, M. G. Papadopoulos, B. Kirtman, J. M. Luis, and R. Zalesny, J. Comput. Chem. **32**, 908 (2011).
[41]B. Skwara, R. W. Gora, R. Zalesny, P. Lipkowski, W. Bartkowiak, H. Reis, M. G. Papadopoulos, J. M. Luis, and B. Kirtman, J. Phys. Chem. A **115**, 10370 (2011).
[42]D. Jacquemin, B. Champagne, and C. Hattig, Chem. Phys. Lett. **319**, 327 (2000); D. Jacquemin, B. Champagne, E. A. Perpete, J. M. Luis, and B. Kirtman, J. Phys. Chem. A **105**, 9748 (2001); B. Champagane, in *Élaboration de Méthodes de CHimie Quantique pour L'evaluation des Hyperpolarisabilités Vibrationnelles-Conséquences pour L'óptique Non linéaire* (PUN, Namur, 2001), p. 68; B. Champagne, M. Spassova, J. B. Jadin, and B. Kirtman, J. Chem. Phys. **116**, 3935 (2002); E. M. Torres, T. L. Fonseca, C. S. Esteves, O. A. V. Amaral, and M. A. Castro, Chem. Phys. Lett. **403**, 268 (2005); W. Niewodniczanski and W. Bartkowiak, J. Mol. Model. **13**, 793 (2007).
[43]B. Champagne, F. A. Bulat, W. T. Yang, S. Bonness, and B. Kirtman, J. Chem. Phys. **125**, 194114 (2006); B. Champagne and M. Spassova, Chem. Phys. Lett. **471**, 111 (2009); B. Kirtman, S. Bonness, A. Ramirez-Solis, B. Champagne, H. Matsumoto, and H. Sekino, J. Chem. Phys. **128**, 114108 (2008); O. Loboda, R. Zalesny, A. Avramopoulos, J. M. Luis, B. Kirtman, N. Tagmatarchis, H. Reis, and M. G. Papadopoulos, J. Phys. Chem. A **113**, 1159 (2009); K. Yoneda, M. Nakano, H. Fukui, T. Minami, Y. Shigeta, T. Kubo, E. Botek, and B. Champagne, ChemPhysChem **12**, 1697 (2011); M. Garcia-Borras, M. Solà, J. M. Luis, and B. Kirtman, J. Chem. Theory Comput. **8**, 2688 (2012).
[44]R. G. Pearson, J. Chem. Educ. **64**, 561 (1987); Z. Zhou and R. G. Parr, J. Am. Chem. Soc. **111**, 7371 (1989); R. G. Parr and P. K. Chattaraj, J. Am. Chem. Soc. **113**, 1854 (1991); R. G. Pearson, J. Chem. Educ. **76**, 267 (1999); M. Torrent-Sucarrat, J. M. Luis, M. Duran, and M. Solà, J. Am. Chem. Soc. **123**, 7951 (2001).